J Electroceram (2006) 17:161–164
DOI 10.1007/s10832-006-5654-4

Dielectric properties of $Pb[(Mg_{1/3}Nb_{2/3}),Ti]O_3$ with Bi modification

Yoon-Sung Kim · Jee-Su Kim · Nam-Kyoung Kim

Received: 29 June 2005 / Revised: 28 September 2005 / Accepted: 21 October 2005

Abstract $Bi(Mg_{2/3}Nb_{1/3})O_3$ was partially substituted into a $Pb(Mg_{1/3}Nb_{2/3})O_3$·$PbTiO_3$ perovskite system and resultant changes in the phase developments and dielectric properties were investigated. Two major structures of columbite and rutile, along with a small fraction of $Mg_4Nb_2O_9$ (α-Al_2O_3 structure), were developed in the B-site precursor system, whereas only a perovskite was observable after the addition of PbO and Bi_2O_3. The replacement of Bi for Pb resulted in a great reduction in the maximum dielectric constants as well as a substantial decrease in the dielectric maximum temperatures.

Keywords Perovskite · Dielectric property · $Pb(Mg_{1/3}Nb_{2/3})O_3$ (PMN) · $PbTiO_3$ (PT) · $Bi(Mg_{2/3}Nb_{1/3})O_3$ (BMN)

1 Introduction

Lead magnesium niobate $Pb(Mg_{1/3}Nb_{2/3})O_3$ (PMN) is a prototype ferroelectric compound, with frequency-dependent dielectric relaxation as well as diffuse phase transition modes. The dielectric constant spectra of PMN possess a maximum value of $\leq$20,000 (1 kHz) at slightly below room temperature [1–3]. Lead titanate $PbTiO_3$ (PT) is a normal ferroelectric, with sharp modes in the phase transition and a very high Curie temperature of 490°C. The two compounds can be readily prepared to a perovskite structure by a so-called "columbite process [4]" and a one-step solid-state reaction, respectively. To the authors' knowledge, however, bismuth magnesium niobate $Bi(Mg_{2/3}Nb_{1/3})O_3$ (BMN) has not been synthesized into a perovskite structure by any means yet [5]. This inability can be attributed to the somewhat small ionic size of Bi [6] to stably fit into the cubo-octahedral sites of a perovskite lattice. The failure can also be attributed to the comparatively strong covalent coupling of Bi-O [7], which leads to a smaller electronegativity difference than the Pb-compound.

PMN and PT form a continuous series of a perovskite solid solution. The PMN·PT pseudobinary system has been studied intensively in many aspects [3, 8–11]. The maximum dielectric constant values of the $(1-x)$PMN·xPT system ranged from 19,900–29,300 (1 kHz) at $x = 0.0$–0.4 [3]. Meanwhile, it was speculated that substitution of Bi for Pb in PMN·PT might bring some interesting results in the perovskite development as well as in dielectric properties, as the chemistry of Pb^{2+} and Bi^{3+} are essentially similar in that the electron configurations are identical except for the slightly heavier nucleus of the latter. In this regard, Pb of the PMN·PT system was partially replaced by Bi, along with simultaneous alterations of the Mg/Nb ratio to compensate for the charge difference between Pb and Bi. However, the substitution amount of BMN was limited to only 10 mol% to suppress the formation of parasitic pyrochlore. System powders were prepared by a B-site precursor method to increase the perovskite yields. Resultant changes in the phase developments and dielectric properties were investigated.

2 Experimental

The 10 mol% $Bi(Mg_{2/3}Nb_{1/3})O_3$-modified $Pb(Mg_{1/3}Nb_{2/3})O_3$·$PbTiO_3$ system can be formulated as $(0.9-x)$Pb$(Mg_{1/3}Nb_{2/3})O_3$·xPbTiO$_3$·0.1Bi$(Mg_{2/3}Nb_{1/3})O_3$, i.e., $(0.9-x)$PMN·xPT·0.1BMN. The values of x ranged from 0.0 to 0.3

Y.-S. Kim · J.-S. Kim · N.-K. Kim (✉)
Department of Inorganic Materials Engineering, Kyungpook National University, Daegu 702-701, Korea
e-mail: nkkim@knu.ac.kr

at regular intervals of 0.1. Starting materials were high-purity chemicals of PbO (> 99.5%), Bi_2O_3 (99.9%), MgO (99.9%), TiO_2 (99.9%), and Nb_2O_5 (99.9%). In order to maintain the compositions as closely to the nominal values as possible, moisture contents of raw chemicals and prepared precursor powders were measured and introduced into the batch calculations.

Powders of the B-site precursor system were separately synthesized from constituent chemicals, Eq. (1), after wet-milling under alcohol using ZrO_2 media, drying, and calcinations at 1000°–1200°C for 2 h. PbO and Bi_2O_3 were added to the precursor powders in stoichiometric proportions, Eq. (2), and the batches were wet-milled, dried, and calcined at 800°C for 2 h. The calcination procedures were repeated once to ensure perovskite formation. Developed structures were examined using the X-ray diffraction (XRD). Prepared powders were granulated with a polyvinyl alcohol binder (2 wt.% aqueous solution) and were isostatically formed into pellets. The preforms were fired for 1 h at 1100°–1200°C in a multiple-enclosure crucible setup [12], with identical composition powders surrounding the pellets to suppress the volatilization of PbO and/or Bi_2O_3 at elevated temperatures. Gold was sputtered on the sintered pellets as electrical contacts. Weak-field (1 V_{rms}/cm) low-frequency (10^3–10^6 Hz) dielectric constant and loss values were measured using an impedance analyzer on cooling.

$$(0.9-x)(Mg_{1/3}Nb_{2/3})O_2 + xTiO_2 + 0.1(Mg_{2/3}Nb_{1/3})O_{1.5} \rightarrow (Mg_{(1.1-x)/3}Ti_xNb_{(1.9-2x)/3})O_{1.95} \quad (1)$$

$$0.9PbO + 0.05Bi_2O_3 + (Mg_{(1.1-x)/3}Ti_xNb_{(1.9-2x)/3})O_{1.95} \rightarrow (Pb_{0.9}Bi_{0.1})(Mg_{(1.1-x)/3}Ti_xNb_{(1.9-2x)/3})O_3 \quad (2)$$

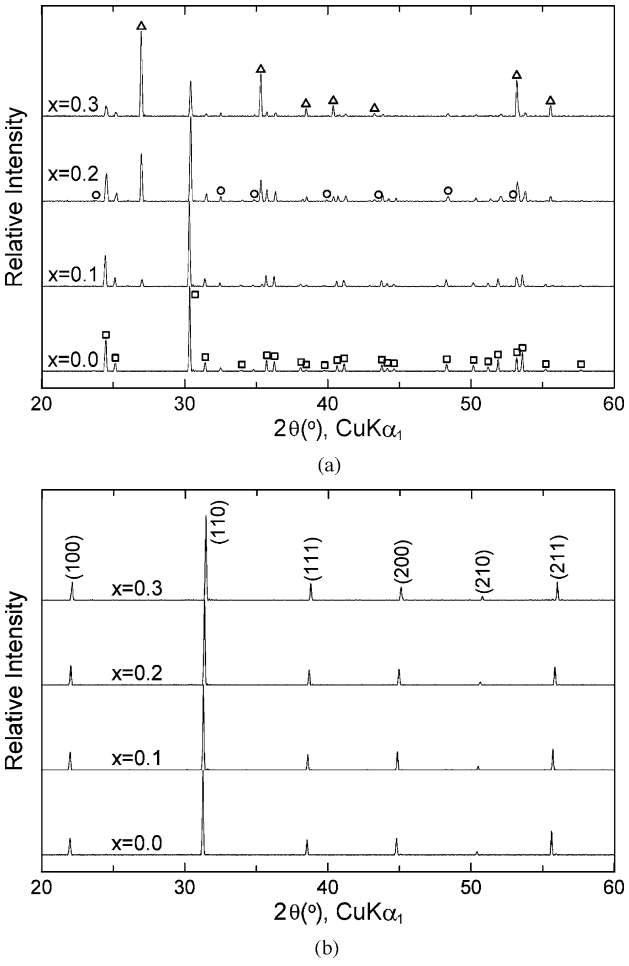

Fig. 1 Room-temperature XRD patterns of the (a) B-site precursor $(0.9-x)(Mg_{1/3}Nb_{2/3})O_2{\cdot}xTiO_2{\cdot}0.1(Mg_{2/3}Nb_{1/3})O_{1.5}$ and (b) perovskite $(0.9-x)$PMN·xPT·0.1BMN systems. (□) columbite, (○) $\alpha-Al_2O_3$, (△) rutile, and (hkl) perovskite

3 Results and discussion

X-ray diffraction results of the B-site precursor system are displayed in Fig. 1(a). Columbite-structured $MgNb_2O_6$ of ICDD No. 33–875 was observed at $x = 0.0$, along with a small fraction of $Mg_4Nb_2O_9$ (α-Al_2O_3 structure, ICDD No. 38-1459). Next, a rutile structure started to develop at $x = 0.1$. The rutile increased further in content to $x = 0.2$ and finally became dominant over the columbite at $x = 0.3$. By careful examination on the diffraction angles, however, the rutile seemed to be not of TiO_2 (ICDD No. 21-1276), but rather of a 1:1 mixture of $[(Mg_{1/3}Nb_{2/3})_{1/2}Ti_{1/2}]O_2$ (ICDD No. 40-366), taking part of the columbite component into solid solution. The $Mg_4Nb_2O_9$ was also present at $x = 0.1$–0.3. Assuming formation of the columbite, rutile, and α-Al_2O_3 structures only, the four compositions investigated can theoretically be resolved as

$$\begin{aligned}
x &= 0.0 : (Mg_{1.1/3}Nb_{1.9/3})O_{1.95} \\
&= 0.9(Mg_{1/3}Nb_{2/3})O_2 + 0.1(Mg_{2/3}Nb_{1/3})O_{1.5} \\
x &= 0.1 : (Mg_{1.0/3}Ti_{0.1}Nb_{1.7/3})O_{1.95} \\
&= 0.7(Mg_{1/3}Nb_{2/3})O_2 + 0.2[(Mg_{1/3}Nb_{2/3})_{1/2}Ti_{1/2}]O_2 \\
&\quad + 0.1(Mg_{2/3}Nb_{1/3})O_{1.5} \\
x &= 0.2 : (Mg_{0.9/3}Ti_{0.2}Nb_{1.5/3})O_{1.95} \\
&= 0.5(Mg_{1/3}Nb_{2/3})O_2 + 0.4[(Mg_{1/3}Nb_{2/3})_{1/2}Ti_{1/2}]O_2 \\
&\quad + 0.1(Mg_{2/3}Nb_{1/3})O_{1.5} \\
x &= 0.3 : (Mg_{0.8/3}Ti_{0.3}Nb_{1.3/3})O_{1.95} \\
&= 0.3(Mg_{1/3}Nb_{2/3})O_2 + 0.6[(Mg_{1/3}Nb_{2/3})_{1/2}Ti_{1/2}]O_2 \\
&\quad + 0.1(Mg_{2/3}Nb_{1/3})O_{1.5}
\end{aligned}$$

The observed intensity ratios between the columbite and rutile are in excellent agreement with those of the analysis. It should be noted that the fraction of the $(Mg_{2/3}Nb_{1/3})O_{1.5}$ (i.e., $Mg_4Nb_2O_9$) stays constant regardless of the composition change, as was actually observed.

X-ray spectra of the system $(0.9 - x)$PMN·xPT·0.1BMN are presented in Fig. 1(b). The patterns of a monophasic perovskite, without any parasitic pyrochlore, indicate that stability of the perovskite was not significantly suppressed by the introduction of 10 mol% BMN. Besides, only fundamental peaks without any superlattice reflections (associated with the perovskite superstructure formation) were observable, indicating the absence of long-range structural ordering, at least in a macroscopic scale, among the octahedral cation species. The diffraction peaks were observed to shift to higher angles with the increase in x, which will be discussed later. Relative densities of the sintered ceramics were 96–97% of the theoretical.

Lattice parameters of the perovskite structure were determined using a Cohen's method [13] on a pseudocubic-symmetry basis and the results are plotted in Fig. 2. The parameter of $x = 0.0$, $(Pb_{0.9}Bi_{0.1})(Mg_{1.1/3}Nb_{1.9/3})O_3$ or 0.9PMN·0.1BMN, was 0.4047 nm, which is almost identical to 0.4046 nm of PMN [3]. The similarity in the values can be explained by approximate balance between two opposite effects: one of a parameter decrease by the increased Bi fraction (vs. Pb) of smaller size and the other of a parameter increase by the increased fraction of larger Mg (vs. Nb) [6] at the A- and B-sites of a perovskite lattice, respectively. Meanwhile, systematic shifts of the diffraction angles to higher values (Fig. 1(b)) resulted in a continuous decrease in the lattice parameters as 0.4036, 0.4033, and 0.4022 nm at $x = 0.1$, 0.2, and 0.3, respectively. The parameter decrease can be easily understood by considering the progressive replacement of the octahedral $Mg_{1.1/3}Nb_{1.9/3}$ complex (weighte-averaged ionic size of 0.0669 nm [6]) by smaller Ti ions of 0.0605 nm [6].

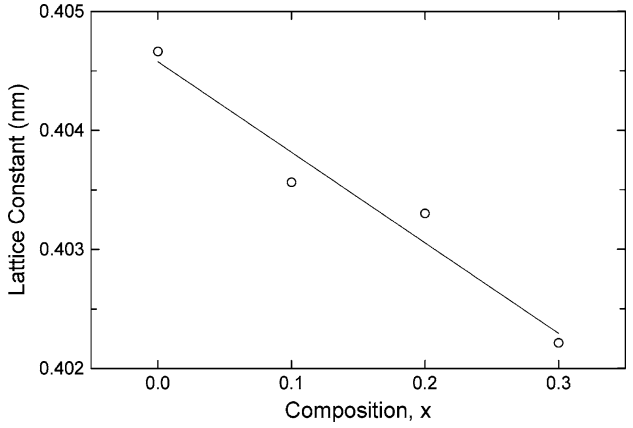

Fig. 2 Dependencies of the perovskite lattice parameter upon composition

Dependencies of the dielectric constant and loss values of a representative composition $x = 0.1$ (0.8PMN·0.1PT·0.1BMN) upon temperature and measurement frequency are shown in Fig. 3, showing well-developed dielectric relaxation behavior with diffuse phase transition modes. Magnitudes of the maximum dielectric constant and corresponding temperatures were 5550 (5°C), 5200 (11°C), 4800 (23°C), and 4350 (35°C) at 1, 10, 100, and 1000 kHz, respectively. Values of the maximum loss (tanδ) were 14.5%, 16.5%, 18.5%, and 22% at the same frequency decades at temperatures of 29–34°C lower than the dielectric maximum temperatures. Frequency-dependent dispersion with diffuse modes in the phase transition was also observed at other compositions of $x = 0.0$, 0.2, and 0.3.

Variations of the maximum dielectric constant (K_{max}) and dielectric maximum temperature (T_{max}) of the system compositions with frequency change are summarized in Fig. 4. The maximum dielectric constants increased steadily with the compositional change: 3300 ($x = 0.0$), 5550 ($x = 0.1$), 6300 ($x = 0.2$), and 8050 ($x = 0.3$) at 1 kHz. However,

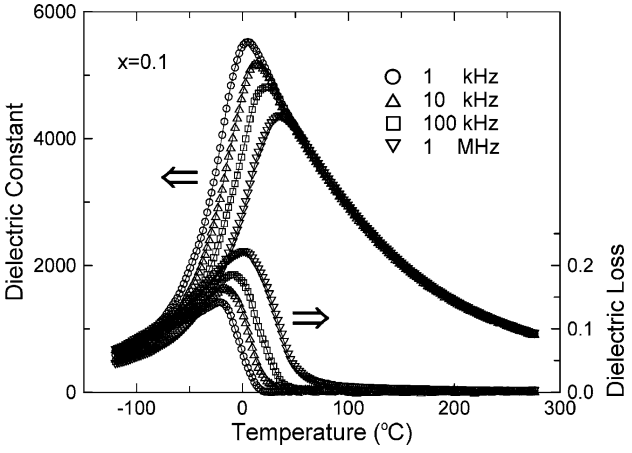

Fig. 3 Representative dielectric constant and loss spectra of $x = 0.1$

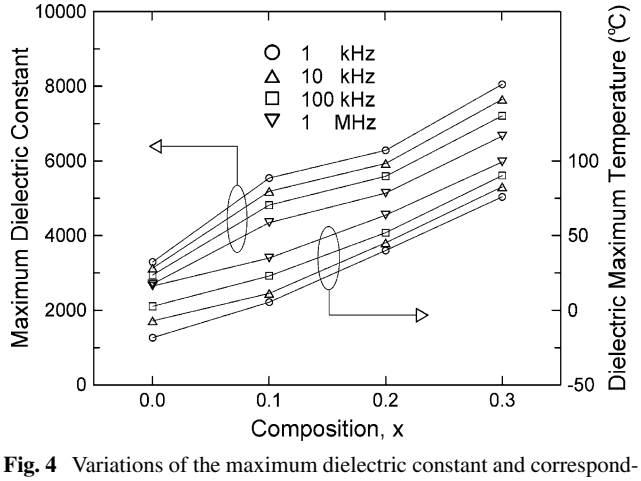

Fig. 4 Variations of the maximum dielectric constant and corresponding temperature with changes in composition and measurement frequency

the values were much smaller than those of the undoped PMN·PT compositions [1, 3], exclusively at low values of x, i.e., PT-poor compositions. The rapid declines in K_{max} seem to be attributable to the breakdown of the long-range dipole interaction by the incorporation of Bi. On the other hand, the comparatively slower reduction rate at high values of x may be interpreted by the substantial recovery of the dipole interaction as a result of the increased PT fraction. Dielectric maximum temperatures of the four investigated compositions were −18, 5, 40, and 76°C 1 kHz. The values were also lower than those of the PMN·PT system, as opposed to the proposed increase [14]. It is interesting to note that the decreases in T_{max} were much steeper at high values of x, where the K_{max}-decreases were slower. Meanwhile, the vaues of ΔT_{max} ($= T_{max,1\ MHz} - T_{max,1\ kHz}$) were 35, 30, 24, and 23°C at $x = 0.0$–0.3, which decreased gradually with the increase in PT concentration.

4 Summary

In the B-site precursor system, columbite $MgNb_2O_6$ was the major structure detected at $x = 0.0$. Rutile started to develop at $x = 0.1$, increased in content at the expense of the columbite at $x = 0.2$, and eventually became dominant at $x = 0.3$. Similar fractions (though of small magnitudes) of the α-Al_2O_3 structure $Mg_4Nb_2O_9$ were also present throughout the composition range of $x = 0.0$–0.3. Semiquantitative analysis on the relative fractions of the three phases were in excellent agreement with the actual observations. After the addition of PbO and Bi_2O_3, in contrast, only a perovskite (without any pyrochlore formation) was identifiable at the investigated composition range. Lattice parameters of the perovskite structure continuously decreased with increasing x. All of the investigated compositions showed typical relaxor behavior of frequency dependence. Both the maximum dielectric constants and the dielectric maximum temperatures increased with an increase in the PT fraction. The two parameters, however, were much smaller than those of the PMN·PT compositions. Besides, the reduction rates in the maximum dielectric constants were faster at low values of x, whereas those in the dielectric maximum temperatures were steeper at high values of x.

Acknowledgment This study was supported by the Korea Research Foundation under Grant No. KRF-2004-002-D00172.

References

1. Y. Yamashita, *Am. Ceram. Soc. Bull.*, **73**(8), 74 (1994).
2. M.-C. Chae, S.-M. Lim, and N.-K. Kim, *Ferroelectrics*, **242**(1–4), 25 (2000).
3. D.-H. Suh, D.-H. Lee, and N.-K. Kim, *J. Eur. Ceram. Soc.*, **22**(2), 219 (2002).
4. S.L. Swartz and T.R. Shrout, *Mater. Res. Bull.*, **17**(10), 1245 (1982).
5. S. Nomura, K. Kaneta, J. Kuwata, and K. Uchino, *Mater. Res. Bull.*, **17**(12), 1471 (1982).
6. R.D. Shannon, *Acta Crystallogr.*, **A32**(5), 751 (1976).
7. A.N. Salak, A.D. Shilin, M.V. Bushinski, N.M. Olekhnovich, and N. P. Vyshatko, *Mater. Res. Bull.*, **35**(9), 1429 (2000).
8. H. Ouchi, K. Nagano, and S. Hayakawa, *J. Am. Ceram. Soc.*, **48**(12), 630 (1965).
9. M. Kuwabara, S. Takahashi, K. Goda, K. Oshima, and K. Watanabe, *Jpn. J. Appl. Phys.*, **31**(9B), 3241 (1992).
10. O. Bunina, I. Zakharchenko, S. Yemelyanov, P. Timonin, and V. Sakhnenko, *Ferroelectrics*, **157**(1–4), 299 (1994).
11. J. Kelly, M. Leonard, C. Tantigate, and A. Safari, *J. Am. Ceram. Soc.*, **80**(4), 957 (1997).
12. M.-C. Chae, N.-K. Kim, J.-J. Kim, and S.-H. Cho, *Ferroelectrics*, **211**(1–4), 25 (1998).
13. B.D. Cullity, *Elements of X-Ray Diffraction* 2nd ed. (Addison-Wesley, Philippines, 1978), p. 363.
14. S.J. Butcher and N.W. Thomas, *J. Phys. Chem. Solids*, **52**(4), 595 (1991).